

Published in final edited form as:

Anesthesiology. 2014 April ; 120(4): 870–879. doi:10.1097/ALN.000000000000107.

Cardioprotection during Diabetes: The Role of Mitochondrial DNA

Maria Muravyeva, M.D., Ph.D.^{*1}, Ines Baotic, M.D.^{*1}, Martin Bienengraeber, Ph.D.^{1,2}, Jozef Lazar, Ph.D.⁴, Zeljko J. Bosnjak, Ph.D.^{1,3}, Filip Sedlic, M.D., Ph.D.¹, David C. Warltier, M.D., Ph.D.^{1,2}, and Judy R. Kersten, M.D.^{1,2}

¹Department of Anesthesiology, Medical College of Wisconsin, Milwaukee, Wisconsin

²Department of Pharmacology and Toxicology, Medical College of Wisconsin, Milwaukee, Wisconsin

³Department of Physiology, Medical College of Wisconsin, Milwaukee, Wisconsin

⁴The Human and Molecular Genetics Center, Medical College of Wisconsin, Milwaukee, Wisconsin

Abstract

Background—Diabetes alters mitochondrial bioenergetics and consequently disrupts cardioprotective signaling. We investigated whether mitochondrial (mt) DNA modulates anesthetic preconditioning (APC) and cardiac susceptibility to ischemia-reperfusion injury using two strains of rats, both sharing nuclear genome of type 2 diabetes mellitus (T2DN) rats and having distinct mitochondrial genomes of Wistar and fawn-hooded hypertensive (FHH) rat strains (T2DN^{mtWistar} and T2DN^{mtFHH}, respectively).

Methods—Myocardial infarct size was measured in Wistar, T2DN^{mtWistar} and T2DN^{mtFHH} rats with or without APC (1.4% isoflurane) in the presence or absence of antioxidant N-acetylcysteine. Flavoprotein fluorescence intensity, a marker of mitochondrial redox state, 5-(and-6)-chloromethyl-2',7'-dichlorofluorescein fluorescence intensity, a marker of reactive oxygen species generation, and mitochondrial permeability transition pore opening were assessed in isolated rat ventricular cardiomyocytes with or without isoflurane (0.5 mmol/L).

Results—Myocardial infarct size was decreased by APC in Wistar and T2DN^{mtWistar} rats (to 42 ± 6%, n = 8; and 44 ± 7%, n = 8; of risk area, respectively) compared to their respective controls (60 ± 3%, n = 6; and 59 ± 9%, n = 7), but not in T2DN^{mtFHH} rats (60 ± 2%, n = 8). N-acetylcysteine applied during isoflurane treatment restored APC in T2DN^{mtFHH} (39 ± 6%, n = 7; and 38 ± 5%, n = 7; 150 and 75 mg/kg N-acetylcysteine, respectively), but abolished protection in control rats (54 ± 8%, n = 6). Similarly to the infarct size data, APC delayed mitochondrial permeability transition pore opening in T2DN^{mtWistar}, but not in T2DN^{mtFHH} cardiomyocytes. Isoflurane increased flavoprotein and 5-(and-6)-chloromethyl-2',7'-dichlorofluorescein fluorescence intensity in all rat strains, with the greatest effect in T2DN^{mtFHH} cardiomyocytes.

Conclusions—Differences in the mitochondrial genome modulate isoflurane-induced reactive oxygen species generation that translates into differential susceptibility to APC and ischemia-reperfusion injury in diabetic rats.

Address correspondence to: Judy R. Kersten, Department of Anesthesiology, Medical College of Wisconsin, 8701 Watertown Plank Road, Milwaukee, Wisconsin 53226. Phone: 414-456-5733, Fax: 414-456-6507, jkersten@mcw.edu.

*The first two authors contributed equally to this work.

Conflict of Interest: The authors declare no competing interests.

Introduction

Evidence for definitive associations between mitochondrial (mt) DNA mutations and the development of diabetes in humans are inconclusive;¹ however, type 2 diabetes is clearly associated with dysfunction in mitochondrial biogenesis and reactive oxygen species (ROS) production.² A recent analysis of the effect of the mitochondrial genome on diabetes and its complications revealed that certain European mtDNA haplogroups were associated with the development of complications of diabetes, whereas, haplogroups did not appear to play a role in the onset of diabetes.¹ Diabetes has been shown to substantially increase the risk of cardiovascular death,^{3, 4} and mitochondria play a central role as effectors of myocardial ischemia and reperfusion (I/R) injury and participate in cardioprotective signaling.⁵ Until now, the role of the mitochondrial genome to modulate susceptibility to I/R injury during diabetes has not been explored, in part, due to the lack of suitable animal models with mtDNA variations. Thus, the current investigation examined the hypothesis that the mitochondrial genome modulates the efficacy of anesthetic preconditioning (APC) with isoflurane through alterations in mitochondrial ROS production using a novel model of type 2 diabetes in rats with mtDNA variations.

Materials and Methods

Animal Model of Type 2 Diabetes

Briefly, the type 2 diabetic (T2DN) models were developed by crossbreeding male Goto Kakizaki rats with female Fawn Hooded Hypertensive (FHH) rats.⁶ The Goto Kakizaki rat is a spontaneously diabetic nonobese Wistar substrain with defective insulin secretion and impaired glucose tolerance, bearing Wistar mtDNA.^{7, 8} The FHH rat is a spontaneous model of renal failure with early systemic, pulmonary and glomerular hypertension, proteinuria, albuminuria and development of focal and segmental glomerulosclerosis, bearing FHH mtDNA.^{9, 10} A cross breeding strategy was used to develop diabetic rats with mtDNA from Wistar (T2DN^{mtWistar}) or FHH (T2DN^{mtFHH}) rats, as previously described.¹¹

Twelve to fourteen-week old male Wistar, T2DN^{mtWistar} and T2DN^{mtFHH} rats¹¹ were obtained from The Human and Molecular Genetics Center (Medical College of Wisconsin, Milwaukee), housed in pairs, and fed a standard Purina 5001 diet (American Institute of Nutrition diet AIN-76A, Teklad, Madison, WI). Tap water was provided *ad libitum*. Baseline fasting glucose levels were increased in both diabetic strains but there were no differences between T2DN^{mtWistar} and T2DN^{mtFHH} rats at 12 wks of age.¹¹ All experimental procedures used in this study were approved by the Animal Care and Use Committee of the Medical College of Wisconsin and conformed to the Guide for the Care and Use of Laboratory Animals.

Myocardial I/R injury *in vivo*

Adult male Wistar or T2DN rats (300 – 360 g) were anesthetized with thiobutabarbital sodium (Inactin, Sigma-Aldrich, St. Louis, MO; 100 mg/kg, intraperitoneal) and additional doses of thiobutabarbital sodium (15 mg/kg) were given during the experiment (1 h after the initial dose) as needed to maintain anesthesia (movement to noxious stimulation). Body temperature was maintained between 36.8° and 37.5°C. The animals were instrumented for the measurement of systemic hemodynamics as previously described.¹² Briefly, heparin-filled catheters were inserted into the right jugular vein and the right carotid artery for fluid administration and measurements of arterial blood pressure, respectively. A tracheotomy was performed, and the trachea was cannulated. Rats were ventilated with positive end-expiratory pressure using an air-and-oxygen mixture. A left thoracotomy was performed in the fifth intercostal space, and the pericardium was opened. A 6-0 prolene ligature was

placed around the proximal left coronary artery and vein in the area immediately below the left atrial appendage. The ends of the suture were threaded through a propylene tube to form a snare. Coronary artery occlusion was produced by clamping the snare onto epicardial surface of the heart with a hemostat and was confirmed by the appearance of epicardial cyanosis. Reperfusion was achieved by loosening the snare and was verified by observing an epicardial hyperemic response. Euthanasia was performed by rapidly extracting the heart. Determination of area at risk (AAR) and myocardial infarct size was done, as described previously.¹³

Myocardial infarct size was measured in Wistar, T2DN^{mtWistar} and T2DN^{mtFHH} rats subjected to 30 min of left coronary artery occlusion and 2 h of reperfusion with or without APC (isoflurane 1.0 minimum alveolar concentration) and in the presence or absence of the ROS scavenger *N*-acetylcysteine (NAC; 75 or 150 mg/kg in 0.9% saline intravenous; Sigma-Aldrich) in six separate experimental groups (fig. 1 and 2).

Isolation of rat ventricular cardiomyocytes

Rats were anesthetized with thiobutabarbital sodium (Inactin, Sigma-Aldrich, 150 mg/kg, intraperitoneal) and hearts were rapidly extracted. Cardiomyocytes were isolated from the hearts of adult male rats by enzymatic dissociation with collagenase type II (Invitrogen, Carlsberg, CA) and protease type XIV (Sigma-Aldrich), as reported previously.¹⁴ After isolation, myocytes were resuspended and stored in Tyrode's solution (in mmol/l: 132 NaCl, HEPES, 5 glucose, 5 KCl, 1 CaCl₂, 1.2 MgCl₂; adjusted to pH 7.4) at room temperature. Cells were allowed to recover from isolation stress for one hour, and experiments were conducted within 5 h of isolation. Only rod-shaped, quiescent cells with distinct cross-striations and preserved membrane integrity were used for experiments. The appropriate volume of isoflurane was dispersed in experimental solution by sonication and delivered to the recording chamber from airtight glass syringes. At the end of each experiment, samples were taken from the outflow of the recording chamber, and experimental isoflurane concentrations were analyzed by gas chromatography (Gas chromatograph GC-8A; Shimadzu, Kyoto, Japan). The mean isoflurane concentration was 0.5 ± 0.06 mmol/l, equivalent to 1 minimum alveolar concentration.

Laser scanning confocal microscopy and image processing

Isolated cardiomyocytes were placed in a polycarbonate recording chamber (Warner Instruments, Hamden, CT) on a confocal microscope stage, and cells were allowed to settle and spontaneously attach to the bottom of the recording chamber for 10 min. Cells were imaged using an inverted laser-scanning confocal microscope (Nikon Eclipse TE2000-U, Tokyo, Japan) with a 60x/1.4 oil-immersion objective (Nikon). Settings of the confocal microscope were consistent in all experimental groups. Fluorescent images were acquired using the EZ-C1 2.10 software (Nikon) and data were analyzed off-line with the MetaMorph 6.2 software (Universal Imaging, West Chester, PA). Results were expressed as percent change in fluorescence intensity relative to baseline (F_0 ; where baseline = 100%).

Flavoprotein fluorescence (FPF) measurements in cardiomyocytes

Mitochondrial redox state was assessed by monitoring native fluorescence intensity of mitochondrial flavoproteins. Isolated cardiomyocytes were superfused with Tyrode's solution in the recording chamber and FPF intensity was recorded by laser-scanning confocal microscopy at room temperature for 24 min, before and after isoflurane exposure for 10 min (fig. 3). The FPF was acquired at the excitation (argon laser) and emission wavelengths of 488 and 500–550 nm, respectively. For the purpose of statistical analyses, the mean fluorescence intensity recorded before (baseline) and during isoflurane exposure was compared.

ROS measurements in cardiomyocytes

ROS formation in isolated cardiomyocytes was monitored using the ROS-sensitive indicator 5-(and-6)-chloromethyl-2',7'-dichlorodihydrofluorescein diacetate, acetyl ester (Invitrogen), which yields fluorescent 5-(and-6)-chloromethyl-2',7'-dichlorofluorescein upon de-esterification and oxidation by ROS. Isolated myocytes were loaded with 2 μ M of 5-(and-6)-chloromethyl-2',7'-dichlorodihydrofluorescein diacetate, acetyl ester dye for 20 min, followed by 7-min washout. Cells were superfused with Tyrode's solution at room temperature and fluorescence intensity from individual cells was monitored by confocal microscopy over 32 min, with isoflurane added at the indicated time (fig. 4). 5-(and-6)-chloromethyl-2',7'-dichlorofluorescein fluorescence was excited with the 488 wavelength of an argon laser, and emission was collected at 500–550 nm by a photomultiplier tube and digitized. Neutral-density filters 4 and 8 (ND4; ND8) were used to minimize dye bleaching. The intensity of baseline fluorescence was compared with the mean fluorescence intensity during isoflurane application.

Mitochondrial permeability transition pore (mPTP) opening measurements in cardiomyocytes

mPTP opening was induced with oxidative stress that was generated by photoexcitation of the fluorescent dye tetramethylrhodamine ethyl ester (TMRE; 100 nmol/l; Invitrogen) in a selected narrowly focused region of cardiomyocytes.^{15–18} Opening of the mPTP was determined by collapse of the mitochondrial membrane potential, indicated by a rapid and complete dissipation of TMRE fluorescence. TMRE fluorescence intensity was acquired using the confocal microscope at excitation (green HeNe laser) and emission wavelengths of 543 and 570–610 nm, respectively. After loading of TMRE for 25 min, the dye was washed out, and a 50 \times 50 μ m recording region of cardiomyocytes was subjected to intensive laser scanning at 3.5 s intervals (fig. 5). The ND4 filter was adjusted to minimize dye bleaching. The arbitrary mPTP opening time was determined as the time to loss of average TMRE fluorescence intensity from the recorded region (excluding nucleus) by half between initial and residual fluorescence intensity. All the confocal microscope settings, laser-scanning intensity and initial TMRE fluorescence intensity were identical in all experimental groups.

Statistical analysis

Data were expressed as mean \pm standard deviation (SD). Comparison of several means was performed using one-way (infarct size) or two-way (hemodynamics) analysis of variance, when appropriate, and the *post-hoc* test used was the Newman-Keuls test. Hemodynamic data were analyzed with repeated measures. For cell experiments, between-group comparisons were performed by one-way ANOVA with the Bonferroni test for *post-hoc* analysis. Changes within and between the groups were considered statistically significant if $P < 0.05$ (two-tailed). Statistical analysis was performed using NCSS 2007 software (Statistical Solutions, Cork, Ireland).

Results

Systemic hemodynamics

Five experiments were excluded from the analysis as a result of technical problems with instrumentation or intractable ventricular fibrillation during coronary artery occlusion and reperfusion (1, T2DN^{mtWistar}; 1, T2DN^{mtFHH}; 1, T2DN^{mtWistar} + NAC; 1, T2DN^{mtFHH} + NAC; 1, T2DN^{mtFHH} + LD NAC). There were no significant differences in baseline systemic hemodynamics among groups (table 1). APC produced similar decreases ($P < 0.05$) in heart rate (HR) and mean arterial pressure (MAP) in each rat strain. NAC alone also decreased HR and MAP in each experimental group. APC produced greater decreases in HR

and MAP in NAC-treated as compared to untreated diabetic rats. Decreases in HR persisted during coronary artery occlusion in NAC-treated rats; however, there was no relationship between HR and myocardial infarct size in any experimental group (data not shown). MAP returned towards baseline values in NAC treated rats during coronary artery occlusion; although, statistically significant decreases in MAP persisted in NAC treated diabetic rats. HR recovered to baseline values after 2 h of reperfusion in Wistar rats, but this did not consistently occur in diabetic rats. MAP was decreased to a similar extent after 2 h of reperfusion in all experimental groups. As previously demonstrated,¹¹ baseline blood glucose concentrations were variable, but similar, in T2DN^{mtWistar} (218 ± 76 ; $n = 13$) and T2DN^{mtFHH} (241 ± 105 mg/dl; $n = 28$) rats.

Mitochondrial genome defines myocardial susceptibility to I/R injury

Body weight, left ventricle (LV) weight and AAR expressed as a percentage of LV weight were similar among groups (table 2). APC significantly ($P < 0.05$) reduced myocardial infarct size (fig. 2) in both Wistar ($42 \pm 6\%$ of the LV AAR, $n = 8$) and T2DN^{mtWistar} rats ($44 \pm 7\%$, $n = 8$), as compared with control experiments ($60 \pm 3\%$, $n = 6$). In contrast, APC did not decrease infarct size in T2DN^{mtFHH} rats ($60 \pm 2\%$, $n = 8$). The ROS scavenger NAC (150 mg/kg) alone decreased infarct size in T2DN^{mtFHH} ($44 \pm 5\%$, $n = 7$) and T2DN^{mtWistar} rats ($41 \pm 9\%$, $n = 7$), and also restored APC in T2DN^{mtFHH} rats ($39 \pm 6\%$, $n = 7$). NAC blocked infarct size reduction during APC in nondiabetic Wistar rats ($54 \pm 8\%$, $n = 6$). To establish that the beneficial effect of NAC was not merely additive to APC, additional experiments were completed at a lower NAC dose (75 mg/kg) that alone had no effect on infarct size in T2DN^{mtFHH} rats ($53 \pm 6\%$, $n = 6$). Low dose NAC was equally effective to restore APC cardioprotection in T2DN^{mtFHH} rats ($38 \pm 5\%$, $n = 7$).

Mitochondrial genome alters mitochondrial redox response to isoflurane

The mitochondrial redox state was assessed by monitoring FPF in isolated cardiomyocytes before and after the administration of isoflurane (fig. 3). Baseline FPF did not differ significantly among Wistar, T2DN^{mtWistar} and T2DN^{mtFHH} cardiomyocytes (fig. 3C). Isoflurane caused an increase in FPF intensity in cardiomyocytes from all three strains, indicating mitochondrial oxidation (fig. 3D); however, isoflurane-induced increases were significantly ($P < 0.05$) greater in T2DN^{mtFHH} ($203 \pm 29\%$ of baseline, $n = 6$) as compared to Wistar ($148 \pm 22\%$, $n = 13$) or T2DN^{mtWistar} ($146 \pm 29\%$, $n = 6$) cardiomyocytes. The decline in FPF to baseline values during washout was delayed in the T2DN^{mtFHH} versus Wistar and T2DN^{mtWistar} cardiomyocytes (fig. 3D).

Mitochondrial genome affects isoflurane-induced ROS generation

T2DN^{mtWistar} and T2DN^{mtFHH} cardiomyocytes exhibited greater ($P < 0.05$) ROS formation (higher 5-(and-6)-chloromethyl-2',7'-dichlorofluorescein fluorescence intensity) at baseline as compared to that observed in cells harvested from Wistar rats (fig. 4); however, there were no differences in ROS generation between diabetic strains at baseline. Isoflurane caused an increase in ROS generation in cardiomyocytes from all three strains. After 24 min of isoflurane exposure, increases in ROS were greatest in T2DN^{mtFHH} ($167 \pm 61\%$ of baseline, $n = 14$) followed by T2DN^{mtWistar} ($107 \pm 28\%$, $n = 17$), and the least in Wistar ($22 \pm 14\%$, $n = 19$) cardiomyocytes (fig. 4D).

Mitochondrial genome affects APC-induced delay in mPTP opening during oxidative stress

mPTP opening was assessed in isolated cardiomyocytes by determining the time to mitochondrial membrane potential collapse in the presence of oxidative stress (fig. 5). APC

significantly ($P < 0.05$) delayed mPTP opening time in T2DN^{mtWistar}, but not in T2DN^{mtFHH} cardiomyocytes (fig. 5C and D).

Discussion

Alterations in mitochondrial genome clearly contribute to the extent of cardiomyocyte death after I/R through the generation of excessive quantities of ROS, calcium overload, and opening of the mPTP.¹⁹ Conversely, exposure to volatile anesthetic agents before ischemia (APC) decreased myocardial injury at the time of reperfusion²⁰ and this effect was, in part, attributable to mitochondria and attenuation of excessive ROS formation at reperfusion.²¹ Preconditioning by isoflurane appears to trigger myocardial protection through an action on mitochondria and subsequent stimulation of prosurvival signaling pathways.^{21, 22} In contrast, hyperglycemia and diabetes^{23–25} abolished the cardioprotective effects of APC, increased oxidative stress, enhanced mPTP opening through modulation of the mitochondrial electron transport chain (ETC),⁵ and abrogated mitochondria-dependent cardioprotection.²⁶ Thus, mitochondria and mitochondrial ROS production appear to function as crucial determinants of susceptibility to myocardial infarction and they are also modulated by volatile anesthetics and diabetes.

The current findings that alterations in mtDNA modulated vulnerability to I/R injury during diabetes and APC confirm and extend previous evidence from our laboratory. Differences in mitochondrial ROS production appeared to underlie strain related differences in diabetic and non-diabetic animals. Diabetes has been shown to be associated with increased myocardial ROS production,²⁷ however, a specific link between mtDNA and susceptibility to myocardial infarction during diabetes has not previously been investigated. Although rats from both diabetic strains exhibited increased glucose levels compared to Wistar rats, only T2DN^{mtWistar} but not T2DN^{mtFHH} rats were protected by APC. The difference in APC response between the two strains was also not explained by differences in baseline cardiac function, as previous characterization demonstrated similar cardiovascular phenotype at 12 weeks of age.¹¹

The efficacy of APC to produce protection in T2DN^{mtFHH} rats was restored by the ROS scavenger NAC, at a dose that had no effect on infarct size alone. In contrast, NAC abolished APC in normal Wistar rats, confirming that small quantities of ROS are required to induce cardioprotective signal transduction during APC,^{13, 21, 28} whereas, excessive ROS during reperfusion contributed to I/R injury. ROS production in vitro was greater in cardiomyocytes harvested from T2DN compared to Wistar rats, consistent with evidence implicating oxidative stress in the pathogenesis of myocardial injury in diabetes. Isoflurane exposure triggered ROS generation during APC *via* interaction with complex I of the ETC^{21, 29} and was greatest in cardiomyocytes from T2DN^{mtFHH} rats. T2DN^{mtFHH} rats share a similar nuclear genome with diabetic T2DN^{mtWistar} rats, but express the mitochondrial genome from FHH rats. Stimulated ROS production was less in T2DN^{mtWistar} as compared with T2DN^{mtFHH} rats, but was lowest in nondiabetic Wistar rats. The mtDNA from T2DN^{mtFHH} rats differs at several locations from that of T2DN^{mtWistar} and Wistar rats. Amino acid modifications in ND2 and ND4, subunits of complex I of the ETC^{11, 30} are present in T2DN^{mtFHH} rats, and activity of complex I is mildly reduced in cardiac mitochondria from T2DN^{mtFHH} compared to T2DN^{mtWistar} rats. APC-induced generation of ROS has been shown to be dependent on isoflurane actions on complex I,²¹ and amino acid alterations in this ETC protein may be responsible for the more pronounced effect of isoflurane on ROS generation during APC in T2DN^{mtFHH} *versus* T2DN^{mtWistar} cardiomyocytes. In contrast to the predominant mtDNA differences between diabetic strains, the results may have suggested that nuclear genome effects contributed to the relatively greater ROS production in diabetic *versus* Wistar cardiomyocytes. Thus, isoflurane-induced

ROS formation is regulated in a complex manner that depends both on mitochondrial and nuclear genome products, and is sensitive to acute anti-oxidant treatment.

Cardiomyocyte oxidation in response to isoflurane was also indicated by the redox state of flavoproteins and was increased in T2DN^{mtFHH} cardiomyocytes, in parallel with pronounced ROS generation. Interestingly, isoflurane-induced flavoprotein oxidation was similar in Wistar and T2DN^{mtWistar} cardiomyocytes. These findings suggested that isoflurane-induced differences in flavoprotein redox state were primarily related to alterations of mtDNA-coded ETC proteins; and are in agreement with previous findings that isoflurane actions on ETC complexes are direct.²⁹ Alterations in ROS production measured with 5-(and-6)-chloromethyl-2',7'-dichlorofluorescein fluorescence are sensitive to ROS produced from multiple sites within cardiomyocytes, including extra-mitochondrial nicotinamide adenine dinucleotide phosphate oxidase that is encoded solely by nuclear and not mitochondrial DNA. In contrast, flavoprotein oxidation reflects the function of ETC proteins that are encoded partly by mitochondrial DNA and are indirectly affected by ROS production. Thus, the finding that flavoprotein oxidation was increased in T2DN^{mtFHH} rats and that these rats were not sensitive to APC supports the contention that mutations in the ETC mediated by the mitochondrial genome are critical determinants of sensitivity of myocardium to protection by APC. Increased oxidation of flavoproteins is likely to be a compensatory response of the electron transfer rate during mitochondrial depolarization and uncoupling caused by isoflurane.^{18, 31} Although mitochondrial K⁺ channels were previously suggested to mediate mitochondrial depolarization by APC and compensatory flavoprotein oxidation,^{27, 32} more recent evidence implied direct effects of isoflurane on the ETC²⁹ as an underlying mechanism for flavoprotein oxidation.

The opening of the mPTP plays a critical role to mediate cardiomyocyte cell death during I/R injury^{33, 34} and mitochondria from diabetic hearts have been shown to be sensitized to mPTP opening.³⁵ Experimental evidence also suggests that delay or prevention of mPTP opening may represent an end-effector of volatile anesthetic-induced cardioprotection.^{36–38} Similarly to the findings *in vivo*, APC was effective to delay mPTP opening in T2DN^{mtWistar} and Wistar cardiomyocytes,^{17, 18} but had no effect in cardiomyocytes harvested from T2DN^{mtFHH} rats. Taken together, the results indicated that mtDNA may importantly modulate the response to I/R injury in diabetes.

Although, HR was decreased by NAC during coronary artery occlusion in both T2DN^{mtWistar} and T2DN^{mtFHH} rats, infarct size was not related to HR or MAP in any experimental group. Thus, it is unlikely that differences in hemodynamics among the groups contributed to the observed results. *In vitro* experiments were performed to elucidate detailed intracellular mechanisms contributing to ROS and mPTP opening in diabetic cardiomyocytes after APC. The genetic strategy employed to investigate the role of mtDNA during APC and diabetes avoids the potential confounding effects of cardiac-specific transgene manipulation, however, ubiquitous mtDNA alterations expressed in cells other than cardiomyocytes could have contributed to the observed results.

In conclusion, the major finding of the study was that differences in the mitochondrial genome in the two diabetic rat strains (T2DN^{mtWistar} versus T2DN^{mtFHH}) conferred a differential sensitivity to APC and susceptibility to I/R injury. This altered sensitivity most likely occurred because of increased ROS production after I/R in the rats bearing the FHH mitochondrial genome. Mitochondrial ROS production and redox state were central in the signaling pathway modulated by diabetes and APC. The results also suggested that mitochondrial proteins could be a therapeutic target for intervention during diabetes to decrease the risk of myocardial injury.

Acknowledgments

The authors would like to thank David Schwabe, B.S., Yasheng Yan, B.S., and Terri L. Misorski, A.A.S., all from the Department of Anesthesiology, Medical College of Wisconsin, Milwaukee, Wisconsin for assistance in completion of this project.

This work was supported by the National Institutes of Health, Bethesda, Maryland (PO1GM066730 to Dr. Kersten, R01HL034708 to Dr. Bosnjak., R01HL098490 to Dr. Bienengraeber).

References

1. Achilli A, Olivieri A, Pala M, Hooshiar Kashani B, Carossa V, Perego UA, Gandini F, Santoro A, Battaglia V, Grugni V, Lancioni H, Sirolla C, Bonfigli AR, Cormio A, Boemi M, Testa I, Semino O, Ceriello A, Spazzafumo L, Gadaleta MN, Marra M, Testa R, Franceschi C, Mitoch Torroni A. Mitochondrial DNA backgrounds might modulate diabetes complications rather than T2DM as a whole. *PLoS One*. 2011; 6:e21029. [PubMed: 21695278]
2. Lowell BB, Shulman GI. Mitochondrial dysfunction and type 2 diabetes. *Science*. 2005; 307:384–7. [PubMed: 15662004]
3. Wang SL, Head J, Stevens L, Fuller JH. Excess mortality and its relation to hypertension and proteinuria in diabetic patients. The world health organization multinational study of vascular disease in diabetes. *Diabetes Care*. 1996; 19:305–12. [PubMed: 8729151]
4. Morrish NJ, Wang SL, Stevens LK, Fuller JH, Keen H. Mortality and causes of death in the WHO Multinational Study of Vascular Disease in Diabetes. *Diabetologia*. 2001; 44(Suppl 2):S14–21. [PubMed: 11587045]
5. Burwell LS, Brookes PS. Mitochondria as a target for the cardioprotective effects of nitric oxide in ischemia-reperfusion injury. *Antioxid Redox Signal*. 2008; 10:579–99. [PubMed: 18052718]
6. Nobrega MA, Fleming S, Roman RJ, Shiozawa M, Schlick N, Lazar J, Jacob HJ. Initial characterization of a rat model of diabetic nephropathy. *Diabetes*. 2004; 53:735–42. [PubMed: 14988259]
7. Kimura K, Toyota T, Kakizaki M, Kudo M, Takebe K, Goto Y. Impaired insulin secretion in the spontaneous diabetes rats. *Tohoku J Exp Med*. 1982; 137:453–9. [PubMed: 6750845]
8. Goto Y, Kakizaki M, Masaki N. Production of spontaneous diabetic rats by repetition of selective breeding. *Tohoku J Exp Med*. 1976; 119:85–90. [PubMed: 951706]
9. Kuijpers MH, Gruys E. Spontaneous hypertension and hypertensive renal disease in the fawn-hooded rat. *Br J Exp Pathol*. 1984; 65:181–90. [PubMed: 6370289]
10. Simons JL, Provoost AP, Anderson S, Troy JL, Rennke HG, Sandstrom DJ, Brenner BM. Pathogenesis of glomerular injury in the fawn-hooded rat: Early glomerular capillary hypertension predicts glomerular sclerosis. *J Am Soc Nephrol*. 1993; 3:1775–82. [PubMed: 8329672]
11. Sethumadhavan S, Vasquez-Vivar J, Migrino RQ, Harmann L, Jacob HJ, Lazar J. Mitochondrial DNA variant for complex I reveals a role in diabetic cardiac remodeling. *J Biol Chem*. 2012; 287:22174–82. [PubMed: 22544750]
12. Ludwig LM, Patel HH, Gross GJ, Kersten JR, Pagel PS, Wartier DC. Morphine enhances pharmacological preconditioning by isoflurane: Role of mitochondrial K(ATP) channels and opioid receptors. *Anesthesiology*. 2003; 98:705–11. [PubMed: 12606915]
13. Ludwig LM, Weihrauch D, Kersten JR, Pagel PS, Wartier DC. Protein kinase C translocation and Src protein tyrosine kinase activation mediate isoflurane-induced preconditioning *in vivo*: Potential downstream targets of mitochondrial adenosine triphosphate-sensitive potassium channels and reactive oxygen species. *Anesthesiology*. 2004; 100:532–9. [PubMed: 15108965]
14. Marinovic J, Bosnjak ZJ, Stadnicka A. Distinct roles for sarcolemmal and mitochondrial adenosine triphosphate-sensitive potassium channels in isoflurane-induced protection against oxidative stress. *Anesthesiology*. 2006; 105:98–104. [PubMed: 16810000]
15. Huser J, Rechenmacher CE, Blatter LA. Imaging the permeability pore transition in single mitochondria. *Biophys J*. 1998; 74:2129–37. [PubMed: 9545072]

16. Zorov DB, Filburn CR, Klotz LO, Zweier JL, Sollott SJ. Reactive oxygen species (ROS)-induced ROS release: A new phenomenon accompanying induction of the mitochondrial permeability transition in cardiac myocytes. *J Exp Med*. 2000; 192:1001–14. [PubMed: 11015441]
17. Pravdic D, Sedlic F, Mio Y, Vlastic N, Bienengraeber M, Bosnjak ZJ. Anesthetic-induced preconditioning delays opening of mitochondrial permeability transition pore *via* protein Kinase C-epsilon-mediated pathway. *Anesthesiology*. 2009; 111:267–74. [PubMed: 19568162]
18. Sedlic F, Sepac A, Pravdic D, Camara AK, Bienengraeber M, Brzezinska AK, Wakatsuki T, Bosnjak ZJ. Mitochondrial depolarization underlies delay in permeability transition by preconditioning with isoflurane: roles of ROS and Ca²⁺. *Am J Physiol Cell Physiol*. 2010; 299:C506–15. [PubMed: 20519447]
19. Baines CP. The mitochondrial permeability transition pore and ischemia-reperfusion injury. *Basic Res Cardiol*. 2009; 104:181–8. [PubMed: 19242640]
20. Kersten JR, Schmelting TJ, Pagel PS, Gross GJ, Warltier DC. Isoflurane mimics ischemic preconditioning *via* activation of K(ATP) channels: Reduction of myocardial infarct size with an acute memory phase. *Anesthesiology*. 1997; 87:361–70. [PubMed: 9286901]
21. Hirata N, Shim YH, Pravdic D, Lohr NL, Pratt PF Jr, Weihrauch D, Kersten JR, Warltier DC, Bosnjak ZJ, Bienengraeber M. Isoflurane differentially modulates mitochondrial reactive oxygen species production *via* forward versus reverse electron transport flow: Implications for preconditioning. *Anesthesiology*. 2011; 115:531–40. [PubMed: 21862887]
22. Zaugg M, Lucchinetti E, Spahn DR, Pasch T, Schaub MC. Volatile anesthetics mimic cardiac preconditioning by priming the activation of mitochondrial K(ATP) channels *via* multiple signaling pathways. *Anesthesiology*. 2002; 97:4–14. [PubMed: 12131097]
23. Kehl F, Krolikowski JG, Mraovic B, Pagel PS, Warltier DC, Kersten JR. Hyperglycemia prevents isoflurane-induced preconditioning against myocardial infarction. *Anesthesiology*. 2002; 96:183–8. [PubMed: 11753019]
24. Tanaka K, Kehl F, Gu W, Krolikowski JG, Pagel PS, Warltier DC, Kersten JR. Isoflurane-induced preconditioning is attenuated by diabetes. *Am J Physiol Heart Circ Physiol*. 2002; 282:H2018–23. [PubMed: 12003806]
25. Amour J, Brzezinska AK, Jager Z, Sullivan C, Weihrauch D, Du J, Vlastic N, Shi Y, Warltier DC, Pratt PF Jr, Kersten JR. Hyperglycemia adversely modulates endothelial nitric oxide synthase during anesthetic preconditioning through tetrahydrobiopterin- and heat shock protein 90-mediated mechanisms. *Anesthesiology*. 2010; 112:576–85. [PubMed: 20124983]
26. Przyklenk K. Efficacy of cardioprotective ‘conditioning’ strategies in aging and diabetic cohorts: The co-morbidity conundrum. *Drugs Aging*. 2011; 28:331–43. [PubMed: 21542657]
27. Boudina S, Sena S, Theobald H, Sheng X, Wright JJ, Hu XX, Aziz S, Johnson JI, Bugger H, Zaha VG, Abel ED. Mitochondrial energetics in the heart in obesity-related diabetes: Direct evidence for increased uncoupled respiration and activation of uncoupling proteins. *Diabetes*. 2007; 56:2457–66. [PubMed: 17623815]
28. Kevin LG, Novalija E, Stowe DF. Reactive oxygen species as mediators of cardiac injury and protection: The relevance to anesthesia practice. *Anesth Analg*. 2005; 101:1275–87. [PubMed: 16243980]
29. Sedlic F, Pravdic D, Hirata N, Mio Y, Sepac A, Camara AK, Wakatsuki T, Bosnjak ZJ, Bienengraeber M. Monitoring mitochondrial electron fluxes using NAD(P)H-flavoprotein fluorometry reveals complex action of isoflurane on cardiomyocytes. *Biochim Biophys Acta*. 2010; 1797:1749–58. [PubMed: 20646994]
30. Schlick NE, Jensen-Seaman MI, Orlebeke K, Kwitek AE, Jacob HJ, Lazar J. Sequence analysis of the complete mitochondrial DNA in 10 commonly used inbred rat strains. *Am J Physiol Cell Physiol*. 2006; 291:C1183–92. [PubMed: 16855218]
31. Minners J, Lacerda L, McCarthy J, Meiring JJ, Yellon DM, Sack MN. Ischemic and pharmacological preconditioning in Girardi cells and C2C12 myotubes induce mitochondrial uncoupling. *Circ Res*. 2001; 89:787–92. [PubMed: 11679408]
32. Nakae Y, Kohro S, Hogan QH, Bosnjak ZJ. Intracellular mechanism of mitochondrial adenosine triphosphate-sensitive potassium channel activation with isoflurane. *Anesth Analg*. 2003; 97:1025–32. [PubMed: 14500152]

33. Garcia-Dorado D, Rodriguez-Sinovas A, Ruiz-Meana M, Inserte J, Agullo L, Cabestrero A. The end-effectors of preconditioning protection against myocardial cell death secondary to ischemia-reperfusion. *Cardiovasc Res.* 2006; 70:274–85. [PubMed: 16635642]
34. Miura T, Tanno M. Mitochondria and GSK-3beta in cardioprotection against ischemia/reperfusion injury. *Cardiovasc Drugs Ther.* 2010; 24:255–63. [PubMed: 20490903]
35. Sloan RC, Moukdar F, Frasier CR, Patel HD, Bostian PA, Lust RM, Brown DA. Mitochondrial permeability transition in the diabetic heart: Contributions of thiol redox state and mitochondrial calcium to augmented reperfusion injury. *J Mol Cell Cardiol.* 2012; 52:1009–18. [PubMed: 22406429]
36. Piriou V, Chiari P, Gateau-Roesch O, Argaud L, Muntean D, Salles D, Loufouat J, Gueugniaud PY, Lehot JJ, Ovize M. Desflurane-induced preconditioning alters calcium-induced mitochondrial permeability transition. *Anesthesiology.* 2004; 100:581–8. [PubMed: 15108972]
37. Venkatapuram S, Wang C, Krolikowski JG, Weihrauch D, Kersten JR, Wartier DC, Pratt PF Jr, Pagel PS. Inhibition of apoptotic protein p53 lowers the threshold of isoflurane-induced cardioprotection during early reperfusion in rabbits. *Anesth Analg.* 2006; 103:1400–5. [PubMed: 17122210]
38. Zhu J, Rebecchi MJ, Tan M, Glass PS, Brink PR, Liu L. Age-associated differences in activation of Akt/GSK-3 β signaling pathways and inhibition of mitochondrial permeability transition pore opening in the rat heart. *J Gerontol A Biol Sci Med Sci.* 2010; 65:611–9. [PubMed: 20427381]

Final Boxed Summary Statement**What we already know about this topic**

- Diabetes is associated with dysfunction in mitochondrial biogenesis and these may contribute to complications from the disease
- Whether the mitochondrial genome participates in the susceptibility to ischemia-reperfusion injury in the heart in the presence of diabetes is unknown

What this article tells us that is new

- Using rat strains and ischemic injury, there was an inferred effect of mitochondrial genome and of mitochondrial function in determining the susceptibility to anesthetic preconditioning and ischemia-reperfusion injury in diabetes

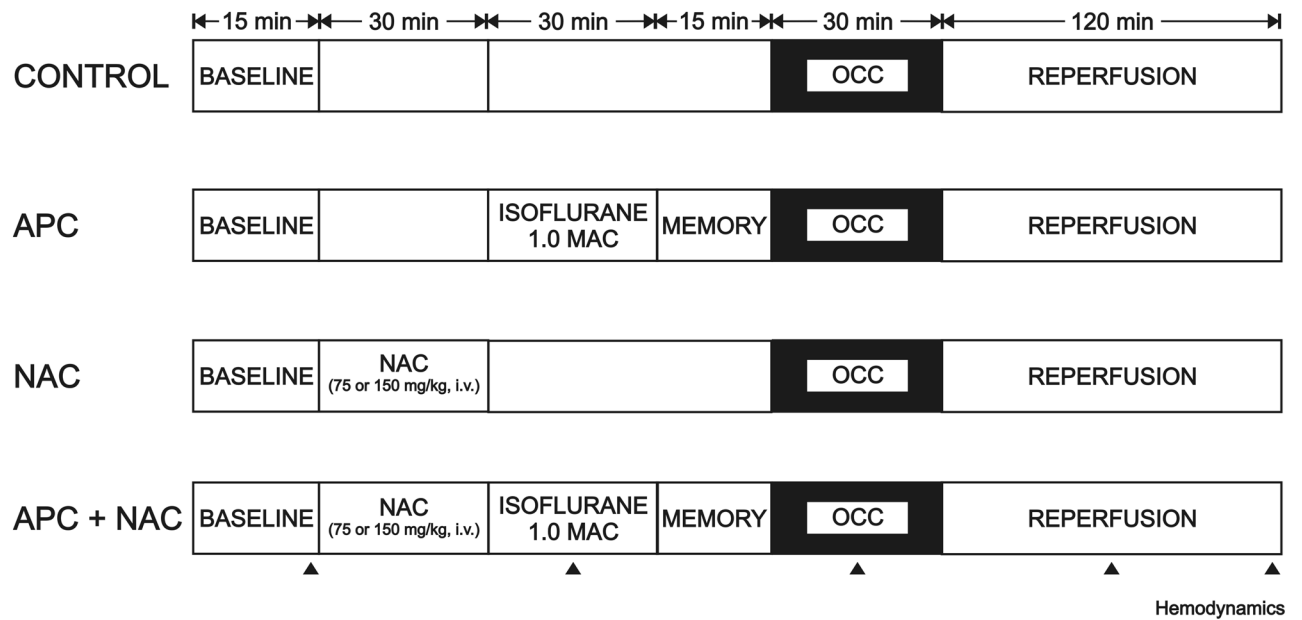


Figure 1.

Schematic diagram depicting the experimental protocols used to determine myocardial infarct size in Wistar and type 2 diabetes mellitus (T2DN) rats *in vivo*. APC = anesthetic preconditioning; MAC = minimum alveolar concentration; NAC = *N*-acetylcysteine; OCC = coronary artery occlusion.

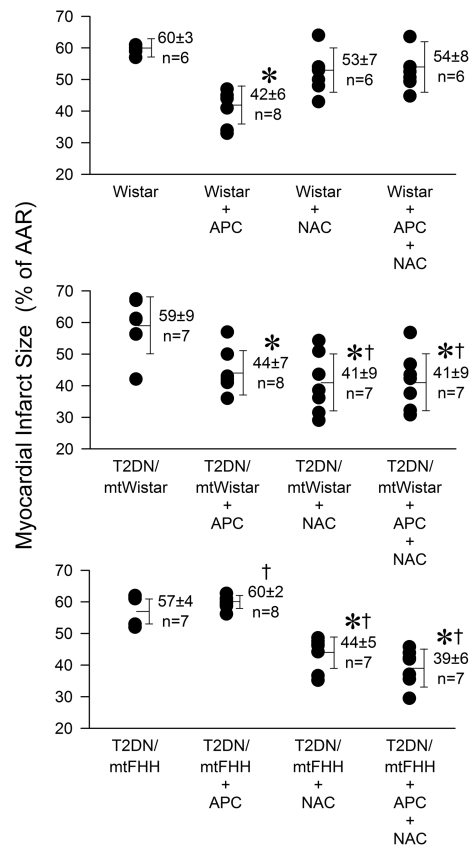
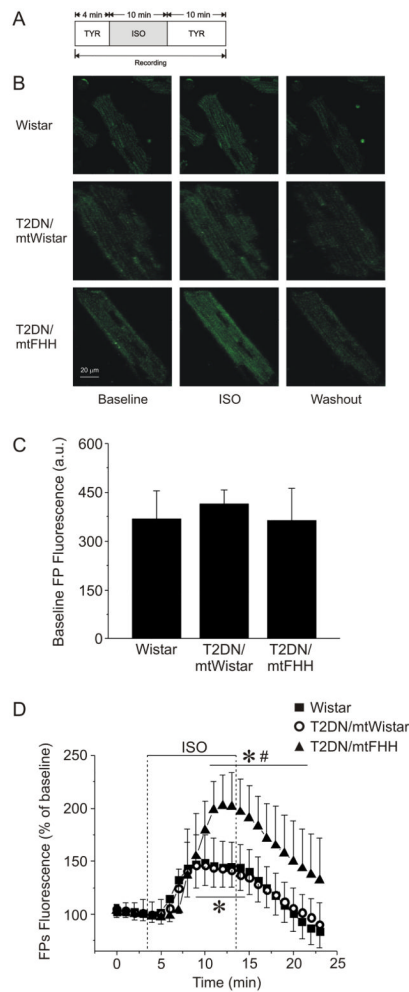


Figure 2.

Myocardial infarct size depicted as a percentage of the area at risk (% of AAR) for infarction in Wistar, type 2 diabetes mellitus (T2DN)^{mtWistar} and T2DN^{mtFHH} rats, respectively. Data are expressed as mean ± SD. * $P < 0.05$ versus respective control without treatment; † $P < 0.05$ versus respective Wistar control. APC = anesthetic preconditioning; FHH = fawn-hooded hypertensive; mt = mitochondrial; NAC = *N*-acetylcysteine

**Figure 3.**

Native fluorescence of flavoproteins (FP) depicted as an indicator of mitochondrial redox state in cardiomyocytes. **(A)** Experimental protocol. **(B)** Representative confocal microscopy images of FP fluorescence in cardiomyocytes before (Baseline), during (ISO) and after (Washout) the addition of 0.5 mmol/l isoflurane. **(C)** Data summary of baseline fluorescence intensity indicates no significant difference between the strains ($P > 0.05$). **(D)** Summarized data of FP fluorescence during ISO exposure and washout expressed as change from the baseline (100%). Isoflurane induced oxidation of mitochondrial flavoproteins in cardiomyocytes isolated from type 2 diabetes mellitus (T2DN)^{mtFHH} rats to a larger extent than in Wistar and T2DN^{mtWistar} cardiomyocytes, respectively. Data are expressed as mean \pm SD, $n = 6$. * $P < 0.05$ versus baseline; # $P < 0.05$ versus Wistar and versus T2DN^{mtWistar}. a.u. = arbitrary units; FHH = fawn-hooded hypertensive; ISO = isoflurane; mt = mitochondrial; TYR = Tyrode solution.

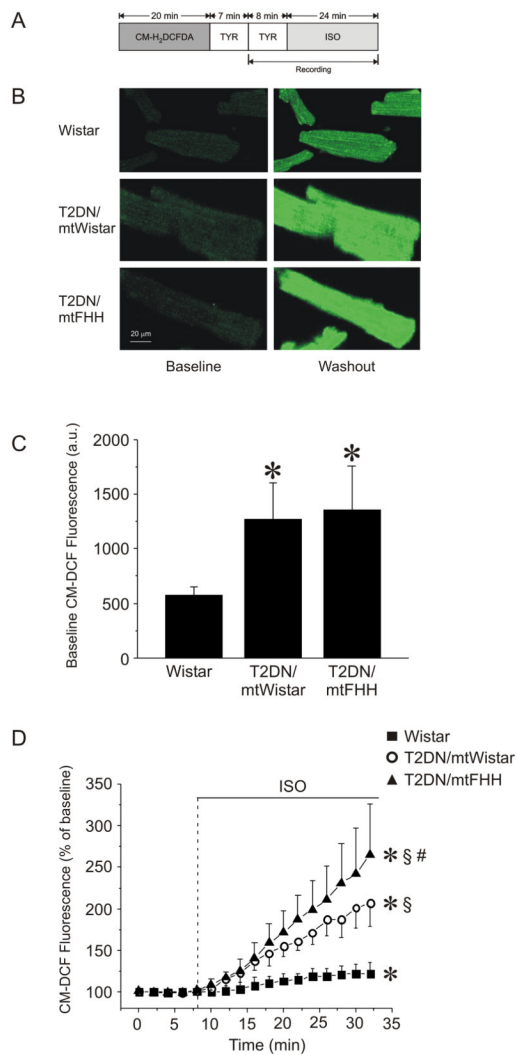
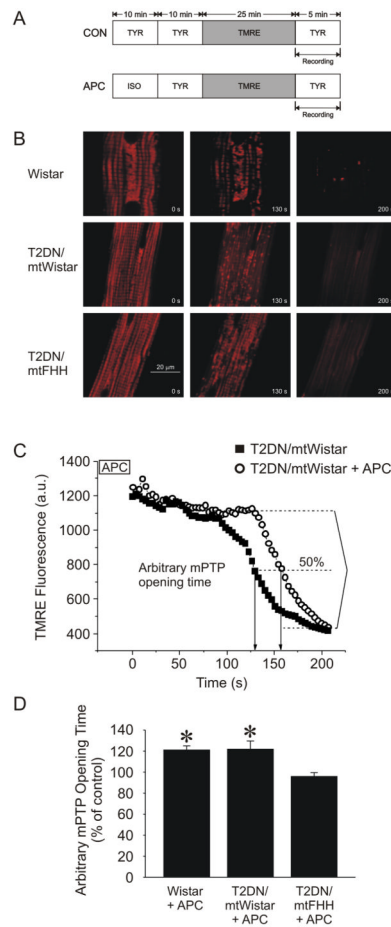


Figure 4. ROS generation in cardiomyocytes as evaluated by 5-(and-6)-chloromethyl-2',7'-dichlorofluorescein (CM-DCF) fluorescence. **(A)** Experimental protocol. **(B)** Representative confocal microscopy images of CM-DCF fluorescence in cardiomyocytes before and after addition of 0.5 mmol/l isoflurane (ISO). **(C)** Quantitative analysis of baseline CM-DCF fluorescence intensity indicates a significant increase in ROS generation in type 2 diabetes mellitus (T2DN) as compared with Wistar strains. **(D)** Time-dependent changes in CM-DCF fluorescence after exposure to ISO. Data are normalized to baseline and presented as mean \pm SD. * $P < 0.05$ versus baseline; § $P < 0.05$ versus Wistar; # $P < 0.05$ versus T2DN^{mtWistar}. a.u. = arbitrary units; CM-H₂DCFDA = 5-(and-6)-chloromethyl-2',7'-dichlorofluorescein diacetate acetyl ester; FHH = fawn-hooded hypertensive; mt = mitochondrial; TYR = Tyrodes solution;.

**Figure 5.**

Opening of the mitochondrial permeability transition pore [mPTP: measured with the mitochondrial potentiometric dye tetramethylrhodamine (TMRE; 100 nmol/l)] after photoexcitation-generated oxidative stress and assessed as rapid and complete mitochondrial depolarization in cardiomyocytes. **(A)** Experimental protocol. **(B)** Representative confocal microscopy images of TMRE fluorescence from a 50 μm^2 region of cardiomyocytes showing mPTP opening in individual mitochondria. **(C)** Arbitrary mPTP opening time expressed as time required to decrease baseline TMRE fluorescence intensity by half (arrows). **(D)** Anesthetic preconditioning (APC) extended the arbitrary mPTP opening time in Wistar, type 2 diabetes mellitus (T2DN)^{mtWistar}, but not in T2DN^{mtFHH} cardiomyocytes. * $P < 0.05$ versus T2DN^{mtFHH}. a.u. = arbitrary units; FHH = fawn-hooded hypertensive; ISO = isoflurane; mt = mitochondrial; TYR = Tyrodes solution.

Table 1

Systemic Hemodynamics

	N	Baseline	Intervention	30 min OCC	Reperfusion	
					1 h	2 h
HR, min⁻¹						
Wistar (Con)	6	365 ± 45	359 ± 40	357 ± 40	353 ± 47	353 ± 40
Wistar + APC	8	378 ± 55	305 ± 73*	377 ± 62	363 ± 56	364 ± 51
Wistar + NAC	6	347 ± 31	309 ± 64*	312 ± 71*	283 ± 66*	274 ± 70*
Wistar + APC + NAC	6	356 ± 25	258 ± 20*†	338 ± 11	324 ± 29	320 ± 40
T2DN ^{mt} Wistar	7	403 ± 20	392 ± 24	414 ± 32	380 ± 42	374 ± 58
T2DN ^{mt} Wistar + APC	8	397 ± 24	300 ± 19*†	384 ± 40	351 ± 44*	348 ± 42*
T2DN ^{mt} Wistar + NAC	7	356 ± 51	312 ± 29*†	324 ± 38*†	304 ± 26*†	322 ± 27*
T2DN ^{mt} Wistar + APC + NAC	7	370 ± 25	259 ± 21*†	324 ± 48*†	305 ± 38*†	311 ± 41*†
T2DN ^{mt} FHH	7	395 ± 48	374 ± 33	399 ± 23	364 ± 29*	345 ± 41*
T2DN ^{mt} FHH + APC	8	404 ± 29	284 ± 30*†§	386 ± 25	354 ± 38*	351 ± 34*
T2DN ^{mt} FHH + NAC	7	332 ± 29§	306 ± 30§	311 ± 26§	303 ± 30§	299 ± 37*
T2DN ^{mt} FHH + LD NAC	6	313 ± 16§	307 ± 34§	307 ± 32§	288 ± 20§	281 ± 25§
T2DN ^{mt} FHH + APC + NAC	7	353 ± 23§	270 ± 33*†§	333 ± 25§	314 ± 13*§	322 ± 20
T2DN ^{mt} FHH + APC + LD NAC	7	339 ± 43§	246 ± 38*†§	326 ± 59§	298 ± 57*§	295 ± 64*
MAP, mmHg						
Wistar (Con)	6	120 ± 19	122 ± 20	123 ± 23	115 ± 21	106 ± 21*
Wistar + APC	8	117 ± 11	66 ± 13*†	109 ± 12	81 ± 21*†	80 ± 21*
Wistar + NAC	6	121 ± 22	96 ± 18*†	109 ± 27	84 ± 27*	89 ± 32*
Wistar + APC + NAC	6	128 ± 19	63 ± 4*†	116 ± 11	97 ± 6*	90 ± 9*
T2DN ^{mt} Wistar	7	134 ± 20	130 ± 24	120 ± 29	92 ± 24*	81 ± 7*
T2DN ^{mt} Wistar + APC	8	141 ± 14	78 ± 27*†	127 ± 12*	87 ± 16*	82 ± 13*

	N	Baseline	Intervention	30 min OCC	Reperfusion	
					1 h	2 h
T2DN ^{mt} Wistar + NAC	7	141 ± 19	104 ± 25 ^{*†}	90 ± 28 [*]	88 ± 13 [*]	81 ± 13 [*]
T2DN ^{mt} Wistar + APC+NAC	7	142 ± 11	48 ± 8 ^{*†‡}	94 ± 25 [*]	69 ± 7 ^{*†}	75 ± 15 ^{*†}
T2DN ^{mt} FHH	7	141 ± 9	133 ± 25	119 ± 19 [*]	90 ± 27 [*]	73 ± 9 ^{*†}
T2DN ^{mt} FHH + APC	8	143 ± 14	62 ± 5 ^{*†‡§}	117 ± 18 [*]	90 ± 24 [*]	79 ± 11 [*]
T2DN ^{mt} FHH + NAC	7	139 ± 18	113 ± 30 ^{*§}	96 ± 28 [*]	81 ± 19 ^{*†}	76 ± 12 ^{*†}
T2DN ^{mt} FHH + LDNAC	6	136 ± 16	139 ± 16	131 ± 21	105 ± 18 [*]	90 ± 19 [*]
T2DN ^{mt} FHH + APC+NAC	7	140 ± 11	47 ± 5 ^{*†‡§}	99 ± 21 [*]	71 ± 14 ^{*†}	72 ± 6 ^{*†}
T2DN ^{mt} FHH + APC + LD NAC	7	135 ± 22	47 ± 4 ^{*†‡§}	118 ± 20 [*]	77 ± 10 ^{*†}	79 ± 16 [*]

Values are mean ± SD. APC = anesthetic preconditioning; Con = control; FHH = fawn-hooded hypertensive; HR = heart rate; LD = low dose (NAC: 75 mg/kg); MAP = mean arterial pressure; mt = mitochondrial; N = number of animals; NAC = N-acetylcysteine (150mg/kg); OCC = coronary artery occlusion; T2DN = type 2 diabetes mellitus.

* significantly ($P < 0.05$) different from Baseline.

[†] significantly ($P < 0.05$) different from respective Wistar (Con) value.

[‡] significantly ($P < 0.05$) different from respective T2DN^{mt}Wistar value.

[§] significantly ($P < 0.05$) different from respective T2DN^{mt}FHH value.

Table 2

Area at Risk for Infarction

	N	BW (g)	LVW (g)	AARLV (%)
Wistar (Con)	6	322 ± 18	0.61 ± 0.05	38 ± 4
Wistar + APC	8	314 ± 27	0.59 ± 0.11	42 ± 10
Wistar + NAC	6	335 ± 13	0.64 ± 0.05	32 ± 10
Wistar + APC + NAC	6	358 ± 21	0.66 ± 0.08	35 ± 7
T2DN ^{mt} Wistar	7	315 ± 37	0.66 ± 0.04	39 ± 4
T2DN ^{mt} Wistar +APC	8	298 ± 48	0.61 ± 0.08	38 ± 6
T2DN ^{mt} Wistar +NAC	7	302 ± 30	0.59 ± 0.08	39 ± 7
T2DN ^{mt} Wistar +APC + NAC	7	325 ± 17	0.62 ± 0.04	39 ± 5
T2DN ^{mt} FHH	7	261 ± 70	0.52 ± 0.1	39 ± 7
T2DN ^{mt} FHH +APC	8	270 ± 65	0.59 ± 0.13	44 ± 5
T2DN ^{mt} FHH +NAC	7	315 ± 13	0.59 ± 0.05	37 ± 3
T2DN ^{mt} FHH +LD NAC	6	326 ± 5	0.63 ± 0.03	36 ± 4
T2DN ^{mt} FHH +APC+ NAC	7	317 ± 19	0.60 ± 0.02	44 ± 5
T2DN ^{mt} FHH +APC + LD NAC	7	314 ± 15	0.61 ± 0.06	40 ± 3

Values are mean ± SD. AARLV = area at risk as a percentage of left ventricle weight; APC = anesthetic preconditioning;; BW = body weight; Con = control; FHH = fawn-hooded hypertensive; LD = low dose (NAC 75 mg/kg); LVW = left ventricle weight; mt = mitochondrial; N = number of animals; NAC = N-acetylcysteine (150 mg/kg); T2DN = type 2 diabetes mellitus.